JPEDAV (2009) 30:136–145
DOI: 10.1007/s11669-009-9469-2
1547-7037 ©ASM International

Diffusion Mobilities in fcc Cu-Au and fcc Cu-Pt Alloys

Yajun Liu, Lijun Zhang, and Di Yu

(Submitted July 8, 2008; in revised form December 10, 2008)

Abundant diffusion data in binary fcc Cu-Au and fcc Cu-Pt alloys have been assessed to obtain the atomic diffusion mobilities of fcc Cu-Au and fcc Cu-Pt alloys by the CALPHAD method. The obtained mobilities are expressed as functions of compositions and temperatures. Good agreements are obtained from comprehensive comparisons between the calculated and experimentally measured self-diffusion coefficients, impurity diffusion coefficients, tracer diffusion coefficients, interdiffusion coefficients, and concentration curves. Accordingly, the developed mobility parameters, in conjunction with the CALPHAD-type thermodynamic descriptions, can be used to simulate diffusion behaviors at high temperatures. It is believed that the results of this work contribute to the design of a general Cu mobility database.

Keywords CALPHAD, Cu-Au, Cu-Pt, diffusion, mobility

1. Introduction

The extensive use of thin films in the fabrication of integrated circuit devices and packaging structures has stimulated widespread interest in studying the interdiffusion for the estimation of reliability. The integrity over long service life of devices incorporating thin metallic layers or coatings depends critically on the diffusion properties of the metallic films. However, depending on the processing procedures or the subsequent operational conditions, interactions between the adjacent thin film layers may occur, which can lead to undesirable performance or degradation of the film properties. To achieve high conductivity, good adherence, and reliable metallurgical stabilities, one of the commonly used approaches is to use a diffusion barrier layer to prevent direct contact between two reactive layers. Examples include Cu/Au, Cu/Pd, Cu/Pt, Cu/Ni, Cu/Co, Cu/Cr, and Cu/Ti bilayer films.[1-3] Therefore, the diffusion barrier approach has played a vital role in the device contact technology and is becoming increasingly important due to the continuing drive toward scaling down the circuit dimensions.

As the CALPHAD thermodynamic technique has made significant progress in practical applications, there is no longer a problem in finding an appropriate thermodynamic description for a specific important binary system. While atomic mobility parameters have recently been developed for the fcc Cu-Ni phase[4] and the fcc Cu-Ag-Sn phase,[5] no work has ever been reported for other Cu-bearing fcc binary phases. Diffusion is a basic and important factor to design and understand many important phenomena, such as precipitation, homogenization, recrystallization, solidification, and protective coatings. As a consequence, there is an increasing need to assess other Cu-bearing binary fcc phases for practical applications. In the CALPHAD assessment procedure for diffusion, mobility parameters of each element in substitutional solution phases are determined from experimental information, including self-diffusion coefficients, impurity diffusion coefficients, tracer diffusion coefficients, intrinsic diffusion coefficients, interdiffusion coefficients, and concentration curves. The development of CALPHAD-type mobility databases is a new research field.[6-9] As a part of efforts to develop a Cu mobility database, this work was undertaken by the CALPHAD method to derive the atomic mobilities of fcc Cu-Au and fcc Cu-Pt alloys as functions of temperatures and compositions.

Yajun Liu, Western Transportation Institute, Montana State University, Bozeman, MT 59715, USA; **Lijun Zhang,** State Key Laboratory of Powder Metallurgy, Central South University, Changsha, Hunan 410083, People's Republic of China; **Di Yu,** American Water Chemicals Inc, Tampa, FL 33619, USA. Contact e-mails: gtg116t@prism.gatech.edu, pcbook@hotmail.com.

2. Diffusion Theory for Binary Systems

For a fictitious binary A-B system, the temporal and spatial evolution of element A is given by the Fick's law in the mass conservation form as below:

$$\frac{\partial C_A}{\partial t} + \nabla \cdot (\vec{J}_A) = 0 \qquad \text{(Eq 1)}$$

where $\vec{J}_A$ and C_A are the flux and volume concentration of element A, respectively; t is time. Because the flux is the measure of how fast atoms can transport, it must be defined within a reference frame. There are three most frequently used reference frames, namely the number-fixed reference frame, the volume-fixed reference frame, and the lattice-fixed reference frame. In diffusion experiments, these reference frames will normally move with respect to one another, and therefore the diffusion fluxes will be different in different reference frames. When the molar volume of a phase is independent of concentrations, the number-fixed reference frame and the volume-fixed reference frame are identical.

The interdiffusion coefficients are defined in the number-fixed reference frame or the volume-fixed reference frame to

characterize how fast different kinds of atoms intermix. The difference between the diffusion rates of constituent elements revealed by the Kirkendall effect can not be interpreted from the interdiffusion coefficients, which leads to the introduction of intrinsic diffusion coefficients to characterize the diffusion of each element. The tracer diffusion coefficients are measured in the absence of chemical composition gradients.

The interdiffusion coefficients are related to the tracer diffusion coefficients by[10]:

$$\tilde{D} = D^{\mathrm{B}}_{\mathrm{AA}} = D^{\mathrm{A}}_{\mathrm{BB}} = (x_{\mathrm{A}} D^{*}_{\mathrm{B}} + x_{\mathrm{B}} D^{*}_{\mathrm{A}}) F \qquad \text{(Eq 2)}$$

where $\tilde{D}$ denotes the interdiffusion coefficient; $D^{\mathrm{B}}_{\mathrm{AA}}$ is the CALPHAD notation of $\tilde{D}$ to show that the flux of element A is induced by the concentration gradient of element A with element B being the dependent element, and $D^{\mathrm{A}}_{\mathrm{BB}}$ can be explained in a similar way; D^{*}_{A} and D^{*}_{B} are the tracer diffusion coefficients of elements A and B, respectively; x_{A} and x_{B} are the molar fractions of elements A and B, respectively; F is the thermodynamic factor to be discussed extensively.

The intrinsic diffusion coefficients are defined in the lattice-fixed reference frame, and they are related to the interdiffusion coefficients through the following equation[11]:

$$\tilde{D} = (x_{\mathrm{A}} D^{\mathrm{I}}_{\mathrm{B}} + x_{\mathrm{B}} D^{\mathrm{I}}_{\mathrm{A}}) \qquad \text{(Eq 3)}$$

where $D^{\mathrm{I}}_{\mathrm{A}}$ and $D^{\mathrm{I}}_{\mathrm{B}}$ are the intrinsic diffusion coefficients defined by $D^{\mathrm{I}}_{\mathrm{A}} = D^{*}_{\mathrm{A}} F$ and $D^{\mathrm{I}}_{\mathrm{B}} = D^{*}_{\mathrm{B}} F$, respectively.

By statistical analysis of the jump frequencies of the atoms situated in the neighborhood of a vacancy, Manning[12] introduced the concept of vacancy wind factor, which accounts for the net flux of vacancies compensating unequal diffusion fluxes in a substitutional alloy. Accordingly, Eq 2 should be amended as:

$$\tilde{D} = (x_{\mathrm{A}} D^{*}_{\mathrm{B}} + x_{\mathrm{B}} D^{*}_{\mathrm{A}}) SF \qquad \text{(Eq 4)}$$

where S is the vacancy wind factor whose limits can be given by[13]:

$$1 \le S \le 1 + \frac{1 - f_0}{f_0} \qquad \text{(Eq 5)}$$

where f_0 is a structure factor (0.781 for fcc and 0.727 for bcc). The limits for S will then be $1 \le S \le 1.28$ for fcc and $1 \le S \le 1.38$ for bcc. The deviation of S from unity is thus not that large, because the interdiffusion coefficients from experiments are frequently scattered to some extent. Therefore, $S = 1$ is used in the CALPHAD treatment.[14,15]

Assuming a mono-vacancy mechanism, the tracer diffusion coefficients can be correlated to the atomic mobilities by[16,17]:

$$D^{*}_{\mathrm{A}} = RTM_{\mathrm{A}} \qquad \text{(Eq 6)}$$

$$D^{*}_{\mathrm{B}} = RTM_{\mathrm{B}} \qquad \text{(Eq 7)}$$

where R is the gas constant; T is the absolute temperature; and M_{A} and M_{B} are the atomic mobilities of elements A and B, respectively.

From the absolute rate theory, the atomic mobility of element i (i = A or B) can be divided into a frequency factor, M^{0}_{i}, and an activation enthalpy, Q_i, by[16-18]:

$$M_i = \frac{1}{RT} \exp\left(\frac{-Q_i + RT \ln(M^{0}_{i})}{RT}\right) = \frac{1}{RT} \exp\left(\frac{\Phi_i}{RT}\right) \qquad \text{(Eq 8)}$$

where Φ_i is a composition-dependent property expressed by the Redlick-Kister polynomials as below:

$$\Phi_i = x_{\mathrm{A}} \Phi^{\mathrm{A}}_{i} + x_{\mathrm{B}} \Phi^{\mathrm{B}}_{i} + x_{\mathrm{A}} x_{\mathrm{B}} \sum_{r} {}^{r}\Phi^{\mathrm{A,B}}_{i} (x_{\mathrm{A}} - x_{\mathrm{B}})^{r} \qquad \text{(Eq 9)}$$

where Φ^{A}_{i},Φ^{B}_{i}, and ${}^{r}\Phi^{\mathrm{A,B}}_{i}$ are the model parameters to be evaluated from experimental data in this work and may vary linearly with respect to temperatures.

The thermodynamic factor in Eq 2 characterizes the deviation of the real system from the corresponding ideal system, and therefore it is the bridge between the tracer diffusion coefficients and the intrinsic diffusion coefficients. The accurate calculation of the thermodynamic factors for a binary system requires accurate thermodynamic information on the desired phase. In the past decades, great effort has been devoted to the thermodynamic assessment of binary systems, and there is no difficulty in obtaining the thermodynamic parameters for common binary systems. For a substitutional solution in the A-B binary system, the molar Gibbs free energies are given by:

$$G_{\mathrm{m}} = x_{\mathrm{A}} {}^{0}G_{\mathrm{A}} + x_{\mathrm{B}} {}^{0}G_{\mathrm{B}} + RT(x_{\mathrm{A}} \ln x_{\mathrm{A}} + x_{\mathrm{B}} \ln x_{\mathrm{B}}) + x_{\mathrm{A}} x_{\mathrm{B}} \sum_{i} {}^{i}L_{\mathrm{A,B}} (x_{\mathrm{A}} - x_{\mathrm{B}})^{i} \qquad \text{(Eq 10)}$$

where ${}^{0}G_{\mathrm{A}}$ and ${}^{0}G_{\mathrm{B}}$ are the molar Gibbs free energies of pure A and B relative to the standard element reference (SER), respectively; the interaction parameters are denoted by ${}^{i}L_{\mathrm{A,B}}$ (i = 0,1,…). Both x_{A} and x_{B} are used in Eq 10 for symmetric purpose. Under such a condition, the thermodynamic factor, denoted by F, is given by[19]:

$$F = \frac{x_{\mathrm{A}} x_{\mathrm{B}}}{RT} \left(\frac{\partial^2 G_{\mathrm{m}}}{\partial^2 x_{\mathrm{A}}} + \frac{\partial^2 G_{\mathrm{m}}}{\partial^2 x_{\mathrm{B}}} - 2 \frac{\partial^2 G_{\mathrm{m}}}{\partial x_{\mathrm{A}} \partial x_{\mathrm{B}}} \right) \qquad \text{(Eq 11)}$$

Alternatively, if x_{B} is eliminated from Eq 10 by $x_{\mathrm{B}} = 1 - x_{\mathrm{A}}$, the corresponding thermodynamic factor can be calculated from[4]:

$$F = \frac{x_{\mathrm{A}}(1 - x_{\mathrm{A}})}{RT} \frac{d^2 G_{\mathrm{m}}}{d^2 x_{\mathrm{A}}} \qquad \text{(Eq 12)}$$

3. Experimental Information

3.1 The Cu-Au System

The impurity diffusion coefficients were reported by various authors. Gorbachev et al.[20] applied ^{195}Au on pure single Cu crystals to measure the impurity diffusion coefficients of Au in Cu by the lathe sectioning method

within 1085 and 1342 K. By means of the sectioning method, Fujikawa et al.[21] measured the impurity diffusion coefficients of ^{198}Au and ^{196}Au in pure single Cu crystals from 633 to 1350 K. Martin et al.[22] utilized the radioactive tracer technique to measure the rate of diffusion of ^{198}Au into polycrystalline Cu from 1023 to 1273 K. Archbold and King[23] measured the impurity diffusion of ^{198}Au in pure polycrystalline Cu from 979 to 1283 K by the utilization of the neutron-activation method. Greenfield and Tweer[24] obtained lattice diffusion coefficients of Au in Cu from the determination of compositional profiles near grain boundaries, where Au diffused from a thin deposit into Cu grain boundaries and an electron diffraction technique was employed to obtain the concentration gradients in the vicinity of the boundaries. Chatterjee and Fabian[25] determined the diffusion rates of Au in both single and polycrystalline Cu in the temperature range 673 to 1323 K using sectioning and irradiation analysis, where there is clear evidence of grain boundary diffusion occurring at and below 1023 K. Vignes and Haeussler[26] investigated the impurity diffusion coefficients of Cu in polycrystalline Au by electron microprobe analysis from 973 to 1179 K, where Cu was vapor deposited to achieve a layer thickness of about 1 micron.

Benci et al.[27] studied the tracer diffusion coefficients of ^{195}Au in fcc Cu-Au alloys with 25 at.% Au. The radioactive ^{195}Au was electroplated onto the specimens, followed by the annealing under purified argon for the penetration experiments. The self-absorption method was adopted for quick measurements of diffusion coefficients. The values of tracer diffusion coefficients of ^{195}Au were reported, which obey the Arrhenius equation. Alexander[28] also investigated the tracer diffusion coefficients of ^{195}Au in Cu-Au alloys with the same composition from 790 to 1210 K. Although the related experimental details are not known, the results of Benci et al.[27] and Alexander[28] are pretty self-consistent. Heumann and Rottwinkel[29] measured the tracer diffusion coefficients of ^{64}Cu and ^{195}Au and interdiffusion coefficients with x_{Au} ranging from 0 to 0.4. The diffusion couples were annealed at 1133 K, after which the diffusion profiles were analyzed by a microprobe. The sectioning method was applied for tracer measurements of ^{195}Au and ^{64}Cu using a precision microtome for sufficient accuracy.

Vignes and Badia[30] measured the interdiffusion coefficients of fcc Cu-Au alloys. The Cu/Au diffusion couples were annealed at 1006, 1016, 1043, and 1130 K for various time. The couples were then sectioned and polished. An electron microanalyzer was used to measure the element concentrations across the diffusion couples. The interdiffusion coefficients were determined by the Matano method. Austin and Richard[31] studied the diffusion of Au into the grain boundaries of Cu bicrystals for both a continuous and an instantaneous source. The concentration contours along the grain boundaries were measured by electron-probe microanalysis. The grain-boundary diffusion coefficients and lattice diffusion coefficients were reported. Ziebold and Ogilvie[32] reported interdiffusion experiments for binary Cu-Au systems at 998 K, where Cu/Au diffusion couples were employed. After interdiffusion, the specimens were subjected to electron microprobe analysis. From the penetration curves, composition-dependent interdiffusion coefficients were calculated with the Boltzmann-Matano analysis. Borovskii et al.[33] studied interdiffusion in polycrystalline Cu/Au diffusion couples at 1059, 993, 867, and 771 K. Electron-microprobe analysis was used to obtain the concentration-penetration curves. The chemical interdiffusion coefficients were calculated with the assistance of the Matano analysis. The temperature dependence of the interdiffusion coefficients was determined and activation energies were calculated. Pinnel and Bennett[34] conducted the interdiffusion experiments with polycrystalline Cu/Au specimens. Interdiffusion temperatures ranged from 1023 down to 773 K. The concentration penetration profiles were obtained from electron-probe micro-analysis, and the interdiffusion coefficients were calculated with the aid of the Matano solution. Unnam et al.[35] measured interdiffusion in Cu-Au binary system with X-ray diffraction and microprobe. The specimens consisted of a 3 μm electrodeposited Au film on a Cu single crystal. The specimens were diffused at 1023 K, after which they were characterized. A finite difference solution to the diffusion equation was used to deduce the concentration dependent chemical diffusion coefficients from the concentration profiles.

3.2 The Cu-Pt System

The self-diffusion coefficients of Pt were measured by various authors. To measure the self-diffusion coefficients of fcc Pt by mechanical sectioning from 1598 to 1873 K, Kidson and Ross[36] applied a mixture of ^{193}Pt, ^{195m}Pt, and ^{197}Pt obtained by neutron activation of pure Pt on polycrystalline fcc Pt. Cattaneo et al.[37] employed ^{195}Pt to determine the self-diffusion coefficients of fcc Pt by surface decrease method from 1523 to 1998 K, where polycrystalline Pt was used. With the sputter sectioning method, the diffusivities of ^{197}Pt in fcc Pt single crystals were measured by Rein et al.[38] from 850 to 1265 K. The impurity diffusion coefficients of Pt in polycrystalline Cu were measured by Fogelson et al.[39] with X-ray diffraction analysis from 1023 to 1348 K. Neumann et al.[40] measured the impurity diffusion coefficients of ^{191}Pt and ^{195}Pt in single crystal Cu by the microtome sectioning method from 1149 to 1352 K.

Johnson and Faulkenberry[41] measured the tracer diffusion coefficients of ^{64}Cu and ^{195m}Pt in pure Cu, pure Pt, and Cu-Pt alloys with 9.8, 24.6, 49.4, and 74.5 at.% Pt. The method used was electrodeposition of the tracer elements followed by diffusion anneals and subsequent lathe-sectioning, counting, etc. The results show that both the Cu and Pt tracer diffusion coefficients decrease with the Pt concentration. Kubaschewski and Ebert[42] applied the diffusion couple technique to measure the interdiffusion coefficients of fcc Cu-Pt alloys. The temperatures employed for the experiments ranged from 1314 to 1674 K, and the interdiffusion coefficients for fcc Cu-Pt alloys with x_{Cu} being 0.139 were reported. Matano[43] determined the interdiffusion coefficients in fcc Cu-Pt alloys by the X-ray method between 763 and 1233 K. The experiments were carried out with the Cu-Pt alloys having 7-10 wt.% Pt, on which Cu was electrodeposited. After annealing, the lattice constants

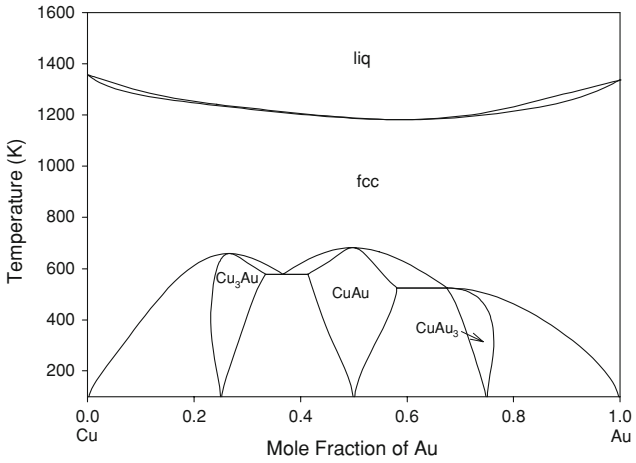

Fig. 1 Calculated Cu-Au phase diagram according to the thermodynamic description of Sundman et al.[45]

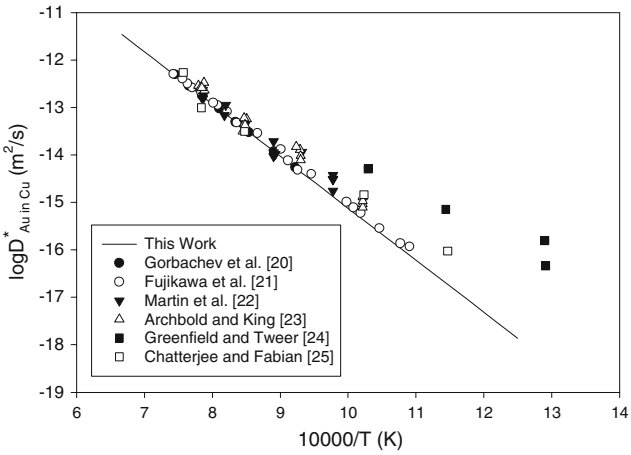

Fig. 2 Comparison between the calculated and experimentally measured impurity diffusion coefficients of Au in fcc Cu

were determined by X-ray photographs which were then correlated with the concentrations. The interdiffusion coefficients were obtained from concentration penetration curves with the error function solution in which the diffusion coefficients were treated as constants.

4. Results and Discussion

In the CALPHAD technique, lower order systems are assessed separately and the obtained parameters are then fixed when advancing to higher order systems. Consequently, the assessment in this work is divided into the following steps. The atomic mobilities for fcc Cu and fcc Au were published by Wang et al.,[4,44] where these mobility parameters were obtained by fitting reported experimental data. Because they can reproduce most of the reported experimental results, those values are adopted in this work as end-members for fcc Cu and fcc Au. The assessment of mobility parameters for the other end-members as well as the interaction parameters is carried out in Comsol Multiphysics by an iterative optimization based on the minimization of the residuals between the calculated and the selected experimental values in the literature. The detailed procedure can be found in our earlier work on the mobility assessment of the Ti-V binary system.[19] In the assessment, the parameters for the end-members will be optimized from self-diffusion coefficients and impurity diffusion coefficients. Once satisfactory agreements for the self-diffusion coefficients and impurity diffusion coefficients are obtained, these parameters are then fixed. The subsequent step is to determine the interaction parameters from the tracer diffusion coefficients and the interdiffusion coefficients. The tracer diffusion coefficients are applied in the first place, because the logarithm of these values and the unknown interaction parameters show a linear relationship. Therefore, the optimization process depends weakly on the provided initial values. When the tracer diffusion coefficients can be well reproduced, the interdiffusion coefficients are then added to the optimization process. Because the parameters obtained by fitting the tracer diffusion coefficients alone can be used as reasonable initial values for the assessment of interdiffusion coefficients, good convergence behaviors are expected.

Table 1 Mobility parameters for the fcc Cu-Au alloys (all in SI units)

Phase	Model	Mobility	Parameters
fcc	$(Au,Cu)_1(Va)_1$	Au	$\Phi^{Au}_{Au} = -176600 - 95.7T$ (a)
			$\Phi^{Cu}_{Au} = -210000 - 79.45T$
			${}^0\Phi^{Au,Cu}_{Au} = 91387.46 - 42.60T$
		Cu	$\Phi^{Cu}_{Cu} = -205872 - 82.5T$ (a)
			$\Phi^{Au}_{Cu} = -167949.99 - 96.29T$
			${}^0\Phi^{Au,Cu}_{Cu} = 74434.63 - 19.23T$

(a) Mobility parameters for self-diffusion of fcc Au and fcc Cu are taken from the work of Wang et al.[4,44]

(b) Thermodynamic parameters are taken from the assessment of Sundman et al.[45] ${}^0L_{Au,Cu} = -28000 + 78.8T - 10T\ln(T)$ and ${}^1L_{Au,Cu} = 6000$

4.1 The Cu-Au System

The thermodynamic description for the Cu-Au binary system was taken from the work of Sundman et al.[45] The mobility parameters for the other two end-members as well as the interaction parameters obtained in this work for fcc Cu-Au alloys are presented in Table 1, where the values from Wang et al.[4,44] are also listed. The calculated Cu-Au phase diagram is presented in Fig. 1, where the fcc phase decomposes at low temperatures to form intermetallics of Cu_3Au, CuAu, and $CuAu_3$. In Fig. 2, the calculated impurity diffusion coefficients of Au in fcc Cu are compared with the experimental data, which lie within a narrow band. The current optimization result is in favor of the values from

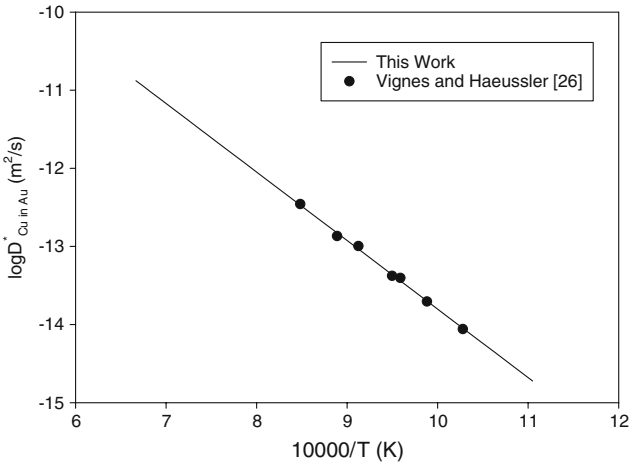

Fig. 3 Comparison between the calculated and experimentally measured impurity diffusion coefficients of Cu in fcc Au

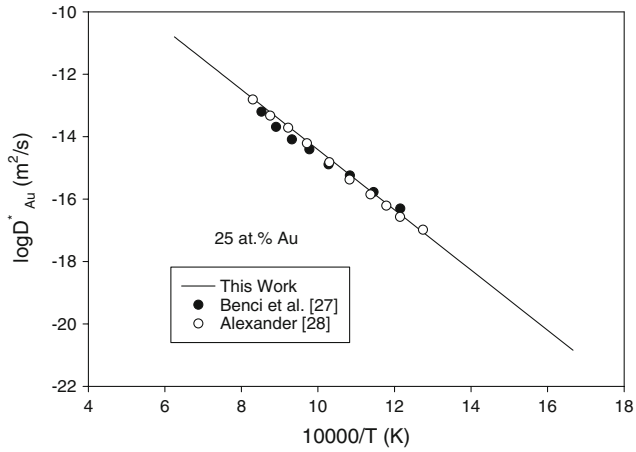

Fig. 4 Comparison between the calculated and experimentally measured Au tracer diffusion coefficients against temperature

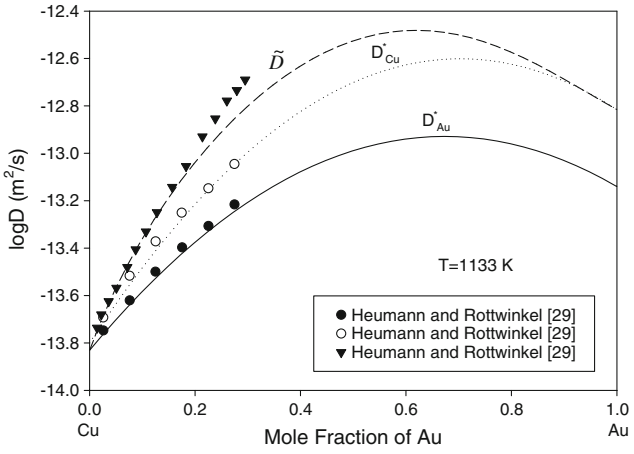

Fig. 5 Comparison between the calculated and experimentally measured various kinds of diffusion coefficients

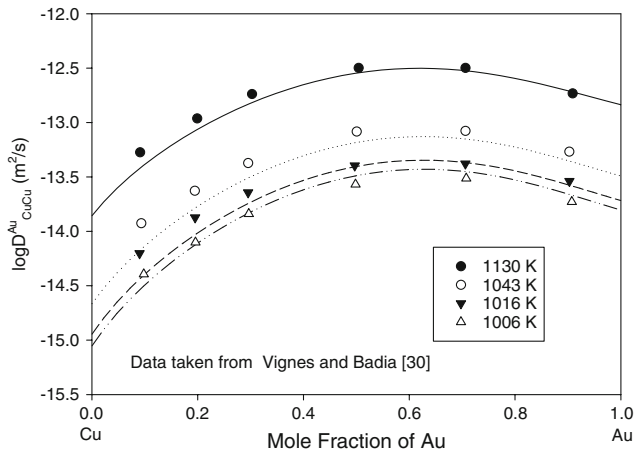

Fig. 6 Comparison between the calculated and experimentally measured interdiffusion coefficients

Gorbachev et al.[20] and Archbold and King.[23] The comparison between the calculated and experimentally measured impurity diffusion coefficients of Cu in fcc Au is given in Fig. 3.

Figure 4 shows the calculated temperature dependence of Au tracer diffusion coefficients in fcc Cu-Au alloys with 25 at.% Au along with the experimental data reported by Benci et al.[27] and Alexander.[28] The calculated tracer diffusion coefficients of Cu and Au as well as the interdiffusion coefficients at 1133 K are presented in Fig. 5 with the experimental values from Heumann and Rottwinkel,[29] where the agreement is satisfactory. The coincidence is not accidental, because the optimization task is to find a compromise between all the data types and sets. In fact, the impurity diffusion coefficients of Au in Cu are the limiting values of the tracer diffusion coefficients of Au as well as the interdiffusion coefficients when $x_{Au} \rightarrow 0$. It is observed that the three kinds of diffusion coefficients peak. The convex feature of the interdiffusion coefficients can be further verified in Fig. 6, where the experimental data from Vignes and Badia[30] are provided. The maximum interdiffusion coefficients at different temperatures are all centered around the same Au concentration of about 0.6. This tendency is consistent with the hypothesis of LeClaire[46] for binary alloys, who stated that an increase in the solute content increases the diffusivity value when it is accompanied by a decrease in the solidus temperature. The Cu-Au phase diagram is characterized by a minimum point on the solidus curve with x_{Au} being around 0.6. As stated earlier, the interdiffusion coefficients are found to peak around $x_{Au} = 0.6$, which is in conformity with the LeClaire's hypothesis[46] within the whole composition range. The calculated interdiffusion coefficients at 1059, 1023, 998, and 867 K are compared with the experimental data from various other authors in Fig. 7, where the results from Ziebold and Ogilive[32] for 998 K can be reasonably reproduced.

To further verify the mobility parameters provided in this work, it is beneficial to simulate the concentration profile within a diffusion couple. In this work, the Au distribution

profile from Heumann and Rottwinkel[29] is used for this purpose. The diffusion couple is made of pure Cu and Cu-Au alloys with 10 at.% Au, which is then annealed at 1133 K for 597,600 s. The governing equation used to predict the Au distribution upon diffusion is Eq 1, and the insulation boundary condition is employed to guarantee that there is no mass flowing inside or outside the simulation domain. The Matano plane is determined from the Au profile of Heumann and Rottwinkel,[29] and this position is used to assign the initial Au concentration, as shown in Fig. 8. The left side of the Matano plane is a Cu-Au alloy and the right side is pure Cu before interdiffusion starts. Comsol Multiphysics features the ability of automatic symbolic differentiation. Therefore, once the molar Gibbs free energy expression is given, the thermodynamic factor can be automatically obtained through Eq 11 or 12. The numerical calculation is performed in Comsol Multiphysics with the finite element method, and evenly distributed 401 grid points are used to achieve good accuracy. The calculated Au distribution is presented in Fig. 8, where the good agreement shows that the mobility parameters obtained in this work can be used for practical diffusion problems at high temperatures.

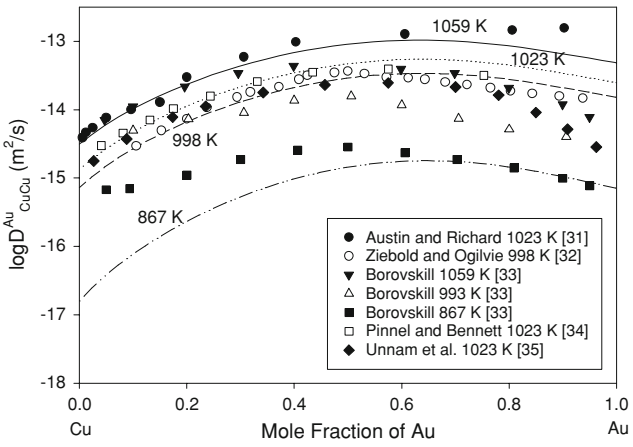

Fig. 7 Comparison between the calculated and experimentally measured interdiffusion coefficients

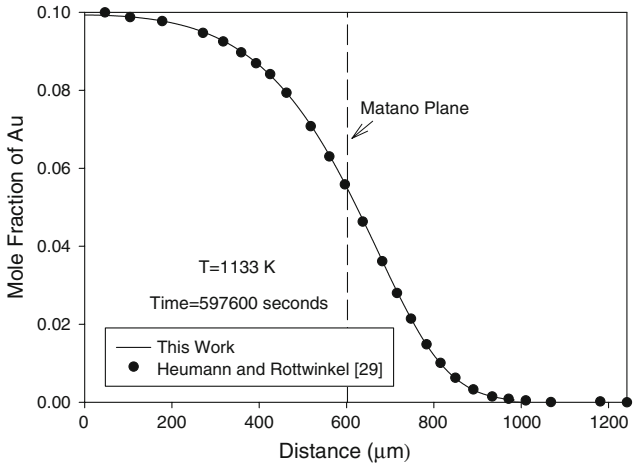

Fig. 8 Comparison between the calculated and experimentally measured Au concentration profile for a Cu/Cu-0.1Au diffusion couple

4.2 The Cu-Pt System

The mobility parameters obtained in this work are presented in Table 2. The calculated Cu-Pt binary phase diagram according to the thermodynamic description of Abe et al.[47] is given in Fig. 9. As can be seen, the Cu-Pt binary phase diagram is very similar to that of the Cu-Au binary system in that the disordered fcc phase transforms into ordered phases at low temperatures. However, the solidus curve increases monotonically with the Pt concentration, which is not consistent with the tendency found in the Cu-Au binary system.

Table 2 Mobility parameters for fcc Cu-Pt alloys (all in SI units)

Phase	Model	Mobility	Parameters
fcc	$(Cu,Pt)_1(Va)_1$	Cu	$\Phi^{Cu}_{Cu} = -205872 - 82.5T$ (a)
			$\Phi^{Pt}_{Cu} = -247993.99 - 99.28T$
			${}^0\Phi^{Cu,Pt}_{Cu} = -30824.75 - 4.12T$
			${}^1\Phi^{Cu,Pt}_{Cu} = 20821.17$
		Pt	$\Phi^{Cu}_{Pt} = -227725.76 - 85.15T$
			$\Phi^{Pt}_{Pt} = -261426.93 - 99.17T$
			${}^0\Phi^{Cu,Pt}_{Pt} = -56673.27 - 5.47T$
			${}^1\Phi^{Cu,Pt}_{Pt} = 65835.60$

(a) Mobility parameters for self-diffusion of fcc Cu are taken from the work Wang et al.[4]

(b) Thermodynamic parameters are taken from the assessment of Abe et al.[47] ${}^0L_{Cu,Pt} = -44105 + 6.53T$, ${}^1L_{Cu,Pt} = -9100 - 1.24T$ and ${}^2L_{Cu,Pt} = 7255 - 8.65T$. (The thermodynamic parameters in Ref. 47 have some problems, and the values presented here were obtained through private communication with the original authors.)

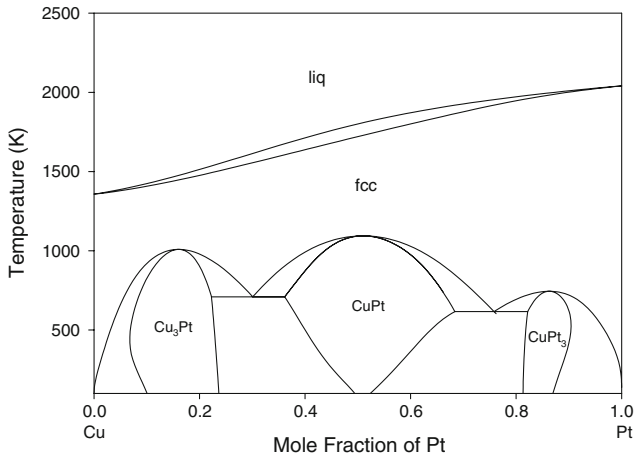

Fig. 9 Calculated Cu-Pt phase diagram according to the thermodynamic description of Abe et al.[47]

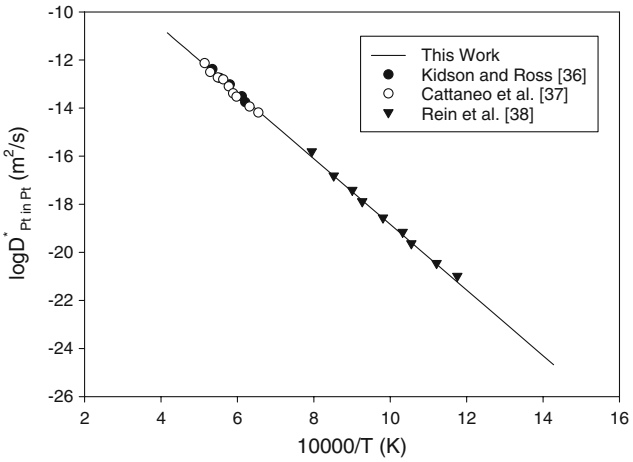

Fig. 10 Comparison between the calculated and experimentally measured self-diffusion coefficients in fcc Pt

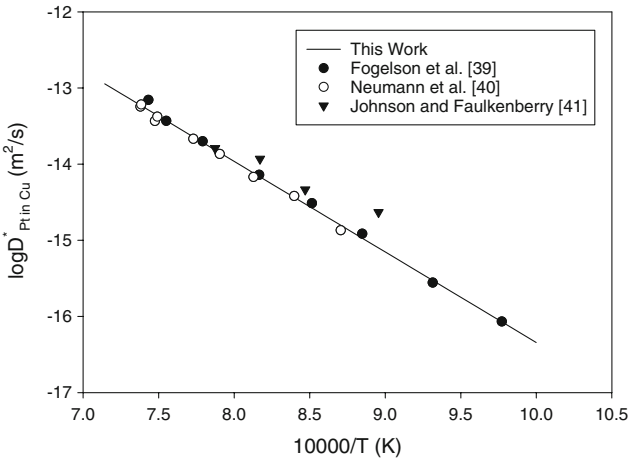

Fig. 11 Comparison between the calculated and experimentally measured impurity diffusion coefficients of Pt in fcc Cu

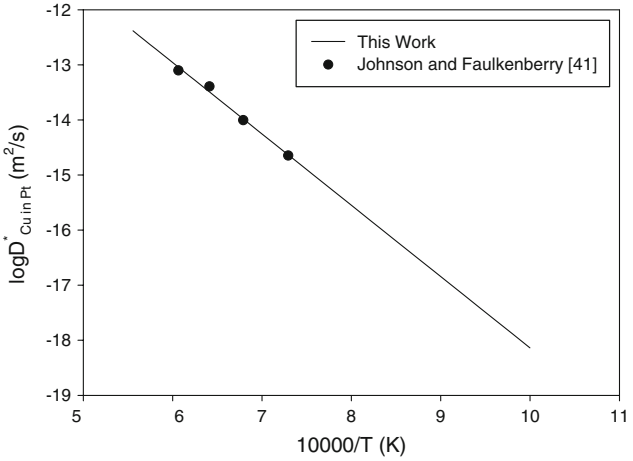

Fig. 12 Comparison between the calculated and experimentally measured impurity diffusion coefficients of Cu in fcc Pt

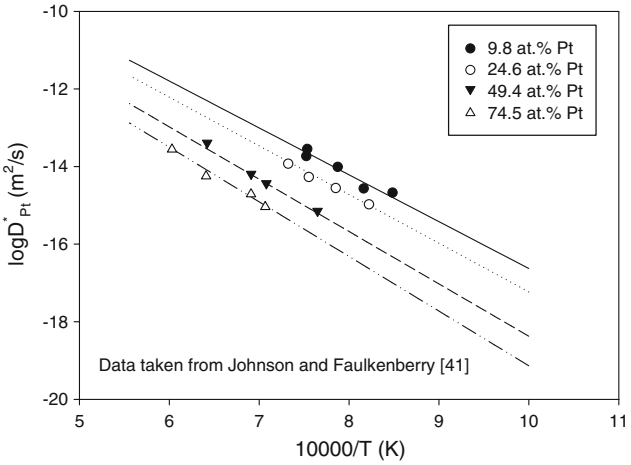

Fig. 13 Tracer diffusion coefficients of Pt in fcc Cu-Pt alloys as a function of reciprocal absolute temperature

In Fig. 10, the calculated self-diffusion coefficients of fcc Pt are compared with the reported experimental data. It is evident that the experimental data from various authors distribute evenly around the calculated line. Figure 11 shows the calculated temperature dependence of impurity diffusion coefficients of Pt in fcc Cu with the reported experimental data, where the calculated values in the present work are in good agreement with the experimental ones. Figure 12 presents the calculated temperature dependence of impurity diffusion coefficients of Cu in fcc Pt along with the experimental results from Johnson and Faulkenberry,[41] where the reported values are consistent with the current results.

Comparisons between the calculated and experimentally measured Cu and Pt tracer diffusion coefficients in various Cu-Pt alloys are presented in Fig. 13 and 14, where the calculated results can well reproduce the reported experimental data from Johnson and Faulkenberry.[41] The reported interdiffusion coefficients for fcc Cu-Pt alloys are rare in the literature. The values from Kubaschewski and Ebert[42] are plotted in Fig. 15 for a comparison with the calculated results, where the calculated interdiffusion coefficients are in reasonable agreement with those experimental data. The interdiffusion coefficients from Matano[43] are plotted with the calculated interdiffusion coefficients for Cu-Pt alloys with 10 and 7 wt.% Pt in Fig. 16, where the good agreement is only evident at high temperatures. The reason for such a dramatic disagreement at low temperatures is not known at present, which may be due to the enhanced grain boundary diffusion at low temperatures or comes from giant experimental errors.

For a comparison with the diffusion coefficients in the Cu-Au system in Fig. 5, the Cu and Pt tracer diffusion coefficients as well as the interdiffusion coefficients are calculated for 1133 K with respect to the Pt concentration, and the results are plotted in Fig. 17. The Cu and Pt tracer diffusion coefficients generally decrease with the Pt concentration except for the Pt tracer diffusion coefficients near

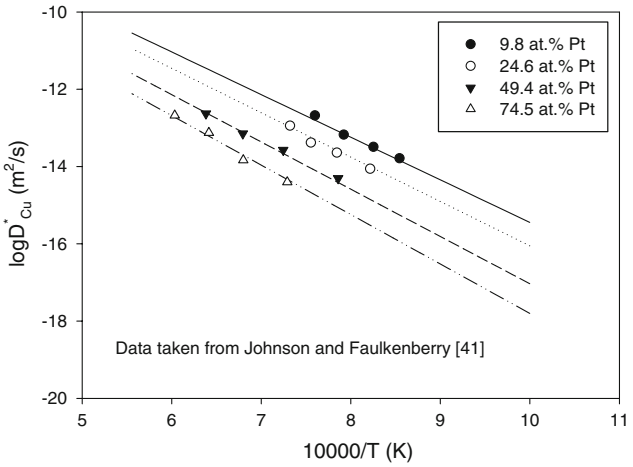

Fig. 14 Tracer diffusion coefficients of Cu in fcc Cu-Pt alloys as a function of reciprocal absolute temperature

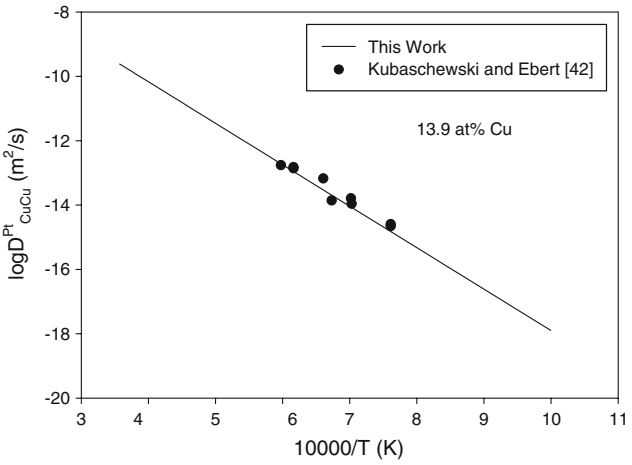

Fig. 15 Comparison between the calculated and experimentally measured interdiffusion coefficients

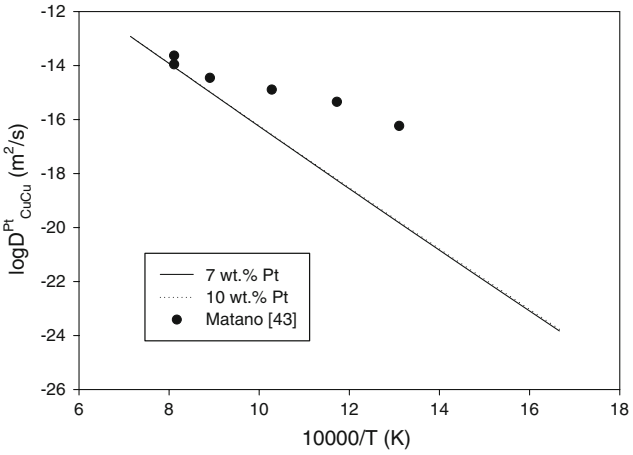

Fig. 16 Comparison between the calculated and experimentally measured interdiffusion coefficients

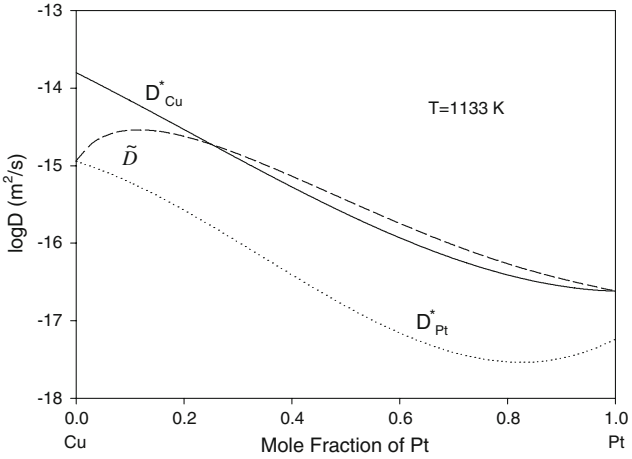

Fig. 17 Calculated tracer diffusion coefficients and interdiffusion coefficients with respect to Pt concentration

the Pt-rich edge where the calculated curve forms a valley. The temperature of the solidus curve for the fcc phase in the Cu-Pt phase diagram increases with the Pt concentration. According to the hypothesis of LeClaire,[46] the interdiffusion coefficients should decrease with the Pt concentration. This prediction is generally valid within the whole composition range except for the Cu-rich edge where the interdiffusion coefficients form a peak.

5. Conclusions

The atomic mobilities in fcc Cu-Au and fcc Cu-Pt alloys have been derived from various experimental data in the literature, including self-diffusion coefficients, impurity diffusion coefficients, tracer diffusion coefficients, interdiffusion coefficients and concentration curves. Good agreements are obtained by comprehensive comparisons between the calculated and experimentally measured data. In conjunction with the CALPHAD thermodynamic description, interdiffusion coefficients at various temperatures and concentration profiles in diffusion couples can be predicted from the developed mobility parameters in this work.

References

1. D.-Y. Shih, C.-A. Chang, J. Paraszczak, S. Nunes, and J. Cataldo, Thin-Film Interdiffusions in Cu/Pd, Cu/Pt, Cu/Ni, Cu/NiB, Cu/Co, Cu/Cr, Cu/Ti, and Cu/TiN Bilayer Films: Correlations of Sheet Resistance with Rutherford Backscattering Spectrometries, *J. Appl. Phys.*, 1991, **70**(6), p 3052-3060

2. H. Ono, T. Nakano, and T. Ohta, Diffusion Barrier Effects of Transition Metals for Cu/M/Si Multilayers (M = Cr, Ti, Nb, Mo, Ta, W), *Appl. Phys. Lett.*, 1994, **64**, p 1511-1513
3. A.N. Aleshin, V.K. Egorov, B.S. Bokstein, and P.V. Kurkin, Study of Diffusion in Thin Au-Cu Films, *Thin Solid Films*, 1993, **223**, p 51-55
4. J. Wang, H.S. Liu, L.B. Liu, and Z.P. Jin, Assessment of Diffusion Mobilities in FCC Cu–Ni Alloys, *Calphad*, 2008, **32**(1), p 94-100
5. G. Ghosh, Dissolution and Interfacial Reactions of Thin-film Ti/Ni/Ag Metallizations in Solder Joints, *Acta Mater.*, 2001, **49**, p 2609-2624
6. C.E. Campbell, W.J. Boettinger, and U.R. Kattner, Development of a Diffusion Mobility Database for Ni-base Superalloys, *Acta Mater.*, 2002, **50**(4), p 775-792
7. C.E. Campbell, A New Technique for Evaluating Diffusion Mobility Parameters, *J. Phase Equilib. Diff.*, 2005, **26**(5), p 435-440
8. Y.W. Cui, K. Oikawa, R. Kainuma, and K. Ishida, Study of Diffusion Mobility of Al-Zn Solid Solution, *J. Phase Equilib. Diff.*, 2006, **27**(4), p 333-342
9. Y.W. Cui, M. Jiang, I. Ohnuma, K. Oikawa, R. Kainuma, and K. Ishida, Computational Study of Atomic Mobility for fcc Phase of Co-Fe and Co-Ni Binaries, *J. Phase Equilib. Diff.*, 2008, **29**(1), p 2-10
10. J. Mimkes and M. Wuttig, Diffusion and Phase Diagram in Binary Alloys, *Thermochim. Acta*, 1996, **282/283**, p 165-173
11. L.E. Trimble, D. Finn, and A. Cosgarea, A Mathematical Analysis of Diffusion Coefficients in Binary Systems, *Acta Metall.*, 1965, **13**, p 501-507
12. J.R. Manning, Diffusion and the Kirkendall Shift in Binary Alloys, *Acta Metall.*, 1967, **15**, p 817-826
13. H. Mehrer, Diffusion in Intermetallics, *Mater. Trans. JIM*, 1996, **37**(6), p 1259-1280
14. J. Andersson and J. Ågren, Models for Numerical Treatment of Multicomponent Diffusion in Simple Phases, *J. Appl. Phys.*, 1992, **72**, p 1350-1355
15. A. Borgenstam, A. Engström, L. Höglund, and J. Ågren, Dictra, a Tool for Simulation of Diffusional Transformations in Alloys, *J. Phase Equilib. Diff.*, 2000, **21**(3), p 269-280
16. T. Helander and J. Ågren, Diffusion in the B2-B.C.C. Phase of the Al-Fe-Ni System-Application of a Phenomenological Model, *Acta Mater.*, 1999, **47**(11), p 3291-3300
17. T. Helander and J. Ågren, A Phenomenological Treatment of Diffusion in Al-Fe and Al-Ni Alloys Having B2-B.C.C. Ordered Structure, *Acta Mater.*, 1999, **47**(4), p 1141-1152
18. B. Jönsson, Assessment of the Mobilities of Cr, Fe and Ni in bcc Cr-Fe-Ni Alloys, *ISIJ Int.*, 1995, **35**(11), p 1415-1421
19. Y. Liu, Y. Ge, D. Yu, T. Pan, and L. Zhang, Assessment of the Diffusional Mobilities in BCC Ti-V Alloys, *J. Alloys Compd.*, 2008, doi:10.1016/j.jallcom.2008.02.111 (in press)
20. V.A. Gorbachev, S.M. Klotsman, Y.A. Rabovskiy, V.K. Talinskiy, and A.N. Timofeyev, Diffusion of Impurities in Copper. V. Diffusion of Gold, Lead and Bismuth in Copper, *Phys. Met. Metall.*, 1977, **44**(1), p 191-194
21. S. Fujikawa, M. Werner, H. Mehrer, and A. Seeger, Diffusion of Gold in Copper over a Wide Range of Temperature, *Mater. Sci. Forum*, 1987, **15-18**, p 431-436
22. A.B. Martin, R.D. Johnson, and F. Asaro, Diffusion of Gold into Copper, *J. Appl. Phys.*, 1954, **25**(3), p 364-369
23. T.F. Archbold and W.H. King, Diffusion of Gold into Copper, *Trans. AIME*, 1965, **233**, p 839-841
24. I.G. Greenfield and I. Tweer, Determination of Compositional Profiles near Grain Boundaries by Electron Diffraction, *Electron Microscopy and Structure of Materials*, *Proc. of the Fifth International Materials Symposium*, G. Thomas, R. M. Fulrath, and R. M. Fisher, Eds., Sept 13-17, 1971 (University of California, Berkeley), University of California Press, Berkeley, 1972, p 236-245
25. A. Chatterjee and D.J. Fabian, Lattice and Grain-Boundary Diffusion of Gold in Nickel, *J. Inst. Met.*, 1968, **96**, p 186-189
26. A. Vignes and J.P. Haeussler, Diffusion of Copper in Gold, *Mem. Sci. Rev. Metall.*, 1966, **63**, p 1091-1094
27. S. Benci, G. Gasparrini, E. Germagnoli, and G. Schianchi, Diffusion of Gold in Cu_3Au, *J. Phys. Chem. Solids*, 1965, **26**, p 687-690
28. W.B. Alexander, "Studies on Atomic Diffusion in Metals; I. Self-Diffusion in the Volume and Along the Dislocations of Cu_3Au; II. Impurity Diffusion in Aluminum and Dilute Aluminum Alloys," Ph.D. Thesis, University of North Carolina, 1969
29. T. Heumann and T. Rottwinkel, Measurement of the Interdiffusion, Intrinsic and Tracer Diffusion Coefficients in Cu-rich Cu-Au Solid Solutions, *J. Nucl. Mater.*, 1978, **69&70**, p 567-570
30. A.V. Vignes and M. Badia, Interdiffusion and Kirkendall Shift in Binary Alloys: Test of the Manning Theory and Influence of the Diffusion Induced Structural Defects on the Interdiffusion Coefficient and Kirkendall Shift, *Diffusion Processes*, *Proc. of the Thomas Graham Memorial Symposium*, J.N. Sherwood, A.V. Chadwick, W.M. Muir, and F.L. Swinton, Eds., Vol. 1, p 275-299
31. A.E. Austin and N.A. Richard, Grain-Boundary Diffusion of Gold in Copper, *J. Appl. Phys.*, 1962, **33**, p 3569-3574
32. T.O. Ziebold and R.E. Ogilvie, Ternary Diffusion in Copper-Silver-Gold Alloys, *Trans. AIME*, 1967, **239**, p 942-953
33. I.B. Borovskii, N.P. Il'in, and E.L. Loseva, Study of Mutual Diffusion in Cu-Au System, *Trudy Inst. Met. A. A. Akad. Nauk SSSR*, 1963, **15**, p 32-40
34. M.R. Pinnel and J.E. Bennett, Mass Diffusion in Polycrystalline Copper/Electroplated Gold Planar Couples, *Metall. Trans.*, 1972, **3**, p 1989-1997
35. J. Unnam, D.R. Tenney, and C.R. Houska, An X-ray Study of Diffusion in the Cu-Au System, *Metall. Trans. A*, 1981, **12**, p 1147-1150
36. G.V. Kidson and R. Ross, *Radioisotopes in Scientific Research: Proceedings of the International Conference* held in Paris in September 1957 under the Auspices of the United Nations Educational Scientific and Cultural Organization, R.C. Extermann, Ed., Vol. 1, p 185-193
37. F. Cattaneo, E. Germagnoli, and F. Grasso, Self-diffusion in Platinum, *Philos. Mag.*, 1962, **7**, p 1373-1383
38. G. Rein, H. Mehrer, and K. Maier, Diffusion of ^{197}Pt and ^{199}Au in Platinum at Low Temperatures, *Phys. Status Solidi A*, 1978, **45**(1), p 253-261
39. R.L. Fogelson, Y.A. Ugai, and A.V. Pokoev, Diffusion of Platinum in Copper, *Fiz. Met. Metalloved.*, 1972, **33**(5), p 1102-1104
40. G. Neumann, M. Pfundstein, and P. Reimers, Diffusion of Platinum in Single Crystals of Silver and Copper, *Philos. Mag. A*, 1982, **45**(3), p 499-507
41. R.D. Johnson and B.H. Faulkenberry, Diffusion Coefficients of Copper and Platinum into Copper Platinum Alloys, Air Force Materials Lab, Wright-Patterson Air Force Base, Ohio, Contract No. AF33(657)-8765, Project No. 7351, Tech. Rept. No. ASD-TDR-63-625, 1963
42. O. Kubaschewski and H. Ebert, Diffusion Measurements in Gold and Platinum Alloys, *Z. Elektrochem.*, 1944, **50**, p 138-144
43. C. Matano, X-ray Studies on the Diffusion of Metals in Copper, *Jpn. J. Phys.*, 1934, **9**, p 41-47

44. J. Wang, L.B. Liu, H.S. Liu, and Z.P. Jin, Assessment of the Diffusional Mobilities in the Face-Centred Cubic Au-Ni Alloys, *Calphad*, 2007, **31**(2), p 249-255
45. B. Sundman, S.G. Fries, and W.A. Oates, A Thermodynamic Assessment of the Au-Cu System, *Calphad*, 1998, **22**(3), p 335-354
46. A. LeClaire, *Progress in Metal Physics*, B. Chalmers, Ed., Butterworth Scientific Publications, London, 1949, p 306-308
47. T. Abe, B. Sundman, and H. Onodera, Thermodynamic Assessment of the Cu-Pt System, *J. Phase Equilib. Diff.*, 2006, **27**(1), p 5-13